Video Article

# Distinguishing Allosteric Effects from Orthosteric Binding in Protein-Ligand Interactions

Arun Chandramohan[1], Srinath Krishnamurthy[1,2], Ganesh S Anand[1]

[1]Department of Biological Sciences, National University of Singapore

[2]Department of Microbiology and Immunology, Rega Institute for Medical Research, KU Leuven

Correspondence to: Ganesh S Anand at dbsgsa@nus.edu.sg

URL: https://www.jove.com/video/56164
DOI: doi:10.3791/56164

Keywords: Protein-ligand interactions, fragment binding, HDXMS, fragment-based drug design, allostery, orthosteric binding, Hsp90

Date Published: 8/8/2017

Citation: Chandramohan, A., Krishnamurthy, S., Anand, G.S. Distinguishing Allosteric Effects from Orthosteric Binding in Protein-Ligand Interactions. *J. Vis. Exp.* (), e56164, doi:10.3791/56164 (2017).

## Abstract

A fundamental challenge in deciphering protein-ligand interactions is distinguishing binding changes at orthosteric sites from the associated allosteric changes at distal sites, as structural data does not always reveal allostery. Ligands mediate both orthosteric and allosteric effects on target proteins and hence, in the context of screening low affinity fragments, it is important to describe fragment efficacy in terms of both direct binding and long-range allosteric responses. This presents a significant problem especially for low affinity ligands. Amide Hydrogen Deuterium Exchange Mass Spectrometry (HDXMS) is a robust method that can provide structural insights and information on conformational dynamics for both high affinity and transient protein-ligand interactions. Here, we describe the use of HDXMS on the ATPase domain of Hsp90, to parse orthosteric and allosteric effects mediated by two high affinity ligands and two low affinity fragment compounds. A comparison of deuterium exchange in ligand-bound-Hsp90 versus apo-Hsp90 was used to describe composite changes that combine both orthosteric effects and allosteric changes. Allostery can be discerned by correlating HDXMS results with structural information about orthosteric binding from crystallographic structures of protein-ligand interactions. Results from this approach indicated that fragments and ligands both mediate interactions at overlapping orthosteric sites but elicit distinct allosteric effects. However, orthosteric interactions of Hsp90 with fragments are inherently weaker due to faster dissociation rates ($k_{off}$). This approach finds important applications in fragment screening, ranking, and lead compound design in fragment-based drug discovery.

## Introduction

Drug development necessitates a complete understanding of the interaction of natural ligands with their target proteins, and utilizes this information to find alternate inhibitors or activators. Traditional drug development pipelines involve a high throughput screening (HTS) strategy to identify lead compounds[1]. An alternative strategy is to use fragments as building blocks for lead compound generation. These have multiple advantages over traditional HTS strategies, including but not limited to, being intellectual property-free, optimizable, and modular[2]. Fragments are defined as small chemical compounds (<300 Da) which mediate fewer than three H-bonding contacts with their target proteins[3]. Fragments are essentially the active moieties of drug molecules. Characterization of fragment-protein interactions poses unique challenges to current structural biology methods due to their low-binding affinities. Another important drawback of structural biology tools, such as X-ray crystallography and cryo-EM, is that they provide insights into kinetically constrained endpoint states which primarily provide information on orthosteric binding contacts between ligands and proteins. This is especially relevant in structures of protein-ligand interactions obtained by soaking ligands with protein crystals, where large-scale conformational movements in solution upon ligand binding, are likely to be undetected. X-ray crystallography also requires extensive optimization for crystallization and only provides a static structure of proteins. However, proteins in solution are dynamic molecules and this dynamics is important for their function[4]. In addition, monitoring proteins in solution offers the additional advantage of capturing transient intermediate changes. Hence, in order to comprehensively map binding effects of ligands to proteins, we need a dynamic overview in addition to the structural information available[5]. Nuclear magnetic resonance (NMR) spectroscopy can provide dynamic structural information but is limited by its analyte size and suffers from sensitivity issues. Additional techniques such as surface plasmon resonance (SPR)[6] and bio-layer interferometry (BLI)[7] can sensitively detect structural changes and capture the binding kinetics of protein-ligand interactions, but do not provide any local structural information. Consequently, capturing dynamic changes in both orthosteric binding sites and allosteric sites, with local structural information and binding kinetics, is critical to provide a systemic model for protein-ligand interactions[8].

Hence, it is essential to work with a more holistic model of protein-ligand interactions, which includes both orthosteric and allosteric changes[9,10]. The large body of available structural information on protein-ligand complexes is limited to details of binding interactions at orthosteric sites. This lack of information on changes at non-orthosteric regions upon ligand binding necessitates a complete description of the changes across the protein in solution. Protein dynamics has been shown to play an important role in distal allosteric communication and modulation, and hence capturing changes in conformational dynamics is crucial to develop a systemic model for ligand binding[11,12] that can be extended to fragment protein interactions. Amide hydrogen-deuterium exchange mass spectrometry (HDXMS) provides a map of the protein dynamics in solution at peptide-resolution, by measuring rates of deuterium uptake at peptide reporters across the protein. HDXMS measures changes in H-bonding and solvent accessibility in backbone amide hydrogens (H-bonding plays a major role in determining deuterium uptake rates) in protein-drug interactions[13]. Since H-bonds play an important role in protein-ligand interactions, HDXMS is uniquely poised to monitor ligand binding[14] and has recently emerged as an important tool for biopharmaceutical discovery and development[15,16,17]. It offers significant advantages in studying

 

protein-ligand complexes, which include no limitations on target protein size, ability to analyze proteins in physiological solution states without the need for concentrated protein samples, two advantages which eliminate artefacts due to aggregation and crowding.

A comparative analysis of deuterium exchange across multiple peptide reporters in the presence and absence of a ligand provides a protein-wide map of the changes in solution dynamics due to ligand binding[18,19]. This offers a read-out of protein dynamics from seconds to longer timescales, determined by the deuterium labelling time[20,21]. HDXMS of protein-ligand complexes reports on both orthosteric changes at the binding site and long-range conformational changes at allosteric sites, in response to ligand binding[22,23]. Overlaying information on protein dynamics with structural data from orthosteric sites enables us to describe long-range conformational changes distal from binding sites. A complete description of both these changes has important applications in describing the interactions of low-affinity fragments with proteins. An approach to map these composite changes involves an initial dynamic description of the natural inhibitors or tight-binding ligands, which provides a standard reference to compare the binding effects of fragments. This initial interaction map of natural ligands acts as the reference fingerprint to compare different fragments to test their binding interactions. The reference fingerprint includes information on the peptide-reporters and magnitude of deuterium uptake changes and kinetics of these changes.

Here, we apply HDXMS to describe orthosteric and allosteric changes in response to the binding of fragments and high-affinity ligands to the N-terminal ATPase domain of Hsp90[24,25,26,27,28]. The protocol focuses initially on Hsp90 and its interactions with two of its high-affinity ligands purified from natural sources: Radicicol[29] and 7-N-Allylamino-17-demethoxygeldanamycin (17-AAG)[30]. The composite changes are differentiated into orthosteric and allosteric changes based on crystallographic structures to identify the regions and HDXMS-specific peptide-reporters that correspond to these respective changes. This information can then be expanded to map the effects of two low affinity fragments, the phenolic compounds, Methyl 3,5-Dihydroxyphenylacetate (Fragment 1) and 2,4 Dihydroxypropiophenone (Fragment 2)[24,31] with dissociation constants of ~500 µM. Further, a workflow is described for the application of this approach to fragment screening for generating a ranking system to sort fragments based on the magnitude of changes in protein dynamics at various loci.

The main advantage of this approach is its wide-applicability to any protein or multi-protein complex. HDXMS studies of proteins have been carried out in various environments, for instance membrane proteins can be characterized in membrane-mimetic nano-discs, detergents, and as assembled macromolecular complexes such as viruses. These highlight the robustness of the approach in describing the dynamics of a wide range of protein targets. HDXMS analyses of the binding of peptide-inhibitors to their target protein offer additional insights into complementary interface residues on the inhibitor end. Since HDXMS involves no disruptive labels, dyes, or specific osmolyte conditions, protein-ligand interactions can be monitored in solution at physiologically similar conditions. These also offer the possibility of studying these interactions with different physical perturbants such as temperature, osmolyte, pH, and other perturbants such as lipids, nucleic acids, and other proteins.

## Protocol

# 1. Preparing $D_2O$ buffer, Quench and Hsp90 Protein Solutions

1. Prepare 100 µM Hsp90 protein solution (expressed in *E. coli* [22]) in Hsp90 aqueous buffer (20 mM HEPES (4-(2-hydroxyethyl)-1-piperazineethanesulfonic acid), 300 mM NaCl, 10% (v/v) glycerol, 0.5 mM TCEP (tris(2-carboxyethyl)phosphine), pH 7.5).
2. Prepare Hsp90 $D_2O$ buffer by vacuum evaporation of the Hsp90 aqueous buffer. Dry the Hsp90 aqueous buffer by vacuum evaporation to remove $H_2O$. Subsequently, reconstitute the dried buffer constituents with an equivalent volume of $D_2O$ to make the Hsp90 $D_2O$ buffer.
    1. pH stability is critical. Ensure that the pH of buffers is stable and measured accurately. Control pH and $pH_{read}$ carefully at each step of the process.
    2. Prepare sufficient aliquots of Hsp90 $D_2O$ buffer for the entire set of experiments from a single buffer solution batch to minimize variability from factors such as pH, temperature, concentrations, and buffer constituents.
    3. Optimize and determine specific temperature, concentrations, and buffer constituents for each protein-ligand system. Refer to[32,33] for in-depth methodological support.

3. Determine deuterium exchange reaction ratios (Ratio of Hsp90 protein solution: ligands in dimethyl-sulfoxide (DMSO): Hsp90 $D_2O$ buffer: Hsp90 quench solution) to achieve the highest deuterium concentration by maximizing the ratio of $D_2O$ buffer.
    1. For Hsp90 deuterium exchange reactions, mix 1 µL of 100 µM Hsp90 protein solution (from step 1.1) with 2 µL of ligand in DMSO/water (for ligand-bound experiments) or 2 µL of DMSO/water-blank (for ligand-free condition) and 27 µL of Hsp90 $D_2O$ buffer (from step 1.2) to achieve a final $D_2O$ concentration of 90% and a final Hsp90 protein concentration of 3.3 µM in a 30 µL deuterium exchange reaction volume.
    2. If needed, concentrate protein solutions prior to initiating the deuterium exchange reaction. For lower concentrations of proteins, use 2 - 4 µL of protein and adjust the deuterium exchange reaction volumes accordingly to obtain the highest $D_2O$ concentration achievable; *e.g.*, increase total reaction volume to 100 - 250 µL.

4. Prepare ligand solutions in water (for high-affinity inhibitors) or DMSO (for low-affinity fragments).
NOTE: The concentrations of ligand solutions are determined to ensure that the ligand concentration saturates the binding site under the final deuterium exchange reaction conditions (step 1.3.1).
    1. Subsequently, for mapping high-affinity inhibitor binding of radicicol and 17-AAG, prepare 300 µM radicicol and 17-AAG inhibitor solutions in DMSO to maintain final deuterium exchange reaction concentrations (step 1.3.1) of radicicol (KD = 19 nM) and 17-AAG (KD = 33 nM)[33] at 20 µM with a final Hsp90 protein concentration of 3.3 µM (6:1 ligand to target protein ratio) to saturate the Hsp90 binding site with inhibitors.
    2. For the low affinity fragments, prepare 75 mM solutions of Fragment 1 and Fragment 2 in DMSO to maintain final deuterium exchange reaction concentrations of Fragment 1 (KD = 490 µM) and Fragment 2 (KD = 570 µM) at 5 mM with a Hsp90 protein concentration of 3.3 µM (~ 1500:1 ligand to target protein ratio) to saturate the Hsp90 binding site with fragments.

5. Prepare the Hsp90 quench solution by adding 2% trifluoroacetic acid (TFA) to water such that addition of 20 µL of Hsp90 quench solution to 30 µL of deuterium exchange reaction (step 1.3.1) reduces the pH of the final quenched exchange reaction to 2.5.

6. Prepare fresh Hsp90 quench solutions before each set of experiments and test their ability to reduce the pH of the final deuterium exchange reaction to 2.5 before every experimental set.
7. Alternatively, use a phosphate buffered quench of pH 2.5 to reduce the pH of the final quenched deuterium exchange reaction to pH 2.5. Ensure that addition of high molarity phosphate buffers does not cause salting out in capillaries.
   NOTE: TFA is preferred as a quench solution for its relative inertness. Estimated time required for preparation of $D_2O$ buffers and Hsp90 quench solution is 3 - 4 hours. Prepared buffers can be stored at 4 °C.

## 2. Setting Up Deuterium Exchange-Liquid Chromatography Coupled to Mass Spectrometry System (LC/MS)

1. Prepare the trapping stage of the LC/MS by adding an online pepsin column and a C18-trap column in a commercial HDX specific module. Maintain the immobilized pepsin at 12 °C and trap column at 4 °C to reduce deuterium back-exchange with solvent.
   NOTE: A simple setup in the absence of a commercial HDX-manager module involves maintaining the trap and C18 columns at 0 to 4 °C (ice-bath or a refrigerator). The quenched sample is then automatically eluted through the pepsin column under high pressure with solvent water at pH 2.5 (by adding formic acid) and the resultant peptides are trapped in a trap column. Another alternative to an inline pepsin column is use of immobilized pepsin-beads for proteolytic cleavage before injection into the trap column.
2. Prepare the analytical stage of the LC/MS by attaching a reverse phase C18 LC column downstream of the trap column such that the trapped peptides are eluted onto the reverse-phase C18 column by a gradient of water:acetonitrile (pH 2.5 by addition of formic acid).
3. Set an LC gradient with three distinct steps: an initial 92:8 water:acetonitrile ratio to remove non-specific peptides, a linear gradient from 92:8 to 15:85 water:acetonitrile ratio, and 15:85 water:acetonitrile ratio to remove any residual peptides or un-cleaved products.
4. Connect the LC outlet to the source of the mass spectrometer.
5. Calibrate the mass spectrometer with reference compounds before data collection (*e.g.,* Glu-fibrinogen peptide or leucine-enkaphalin solutions). Add the reference compound solutions to the mass spectrometer and select 'continuous calibration' mode during data collection. Collect mass spectrometry data in MS/MS mode for data independent analysis (DIA).
   NOTE: Data collection automatically collects precursor ion and fragment ion spectra along with the retention time of individual precursor ions.
6. Modify trapping time for pepsin proteolysis, LC gradient, and elution time to improve sequence coverage, if required.
   NOTE: The experimental setup, peptide identification, and deuterium exchange have also been previously described[22,32]. This representative LC/MS setup described for Hsp90 can be directly applicable for non-aggregating homogenous protein samples. The estimated time required for preparation of solutions, columns, and the calibration of the mass spectrometer (MS) is around 2 - 3 hours.

## 3. Determining Peptide-List from Undeuterated Hsp90 LC/MS Experiments

1. Prepare undeuterated reactions of ligand-free Hsp90 by mixing 1 µL of Hsp90 protein solution (step 1.1) + 2 µL DMSO-blank + 27 µL of Hsp90 aqueous buffer. Add 20 µL of Hsp90 quench solution (step 1.5) to reduce the pH of the solution to 2.5.
2. Inject this sample into the HDX-manager fitted with pepsin, trap, and C18 columns with outlets to a mass spectrometer (steps 2.1 to 2.5). Press the 'start' button in the HDX-manager to start pepsin-proteolysis followed by mass spectrometry data collection during LC gradient.
3. Obtain the peptide-database (theoretical list of all possible peptides) using the protein primary sequence and the proteolytic enzyme used for cleavage (pepsin)[34,35] using the vendor provided[34,35] or other integrated analysis software[37,38].
4. Search for peptides identifiable in the sample against the peptide-database using the MS/MS mass spectrometry data from the undeuterated Hsp90 protein experiments (step 3.1).
5. Identify and collect a list of peptides along with their LC retention times from precursor and fragmentation profiles obtained simultaneously throughout the LC gradient [36].
6. Filter the peptide-list to remove peptides with low intensity, poor fragmentation profiles, and high error. Typically use cut-offs, in validated or vendor-provided software[37,38,39], to select peptides with minimum peak intensity of 2,000 Arbitrary Units (AU), maximum MH+ error of 10 ppm and a minimum of one fragment.
7. Filter the peptide list to ensure that peptides that were eluted only during the gradient (step 2.3) are selected, to maintain reproducibility in obtaining a final peptide list.

## 4. Additional Optimization

1. Add additional post-quench reagents such as denaturants in quench solution (urea and guanidine hydrochloride) and repeat steps 3.1 to 3.7 to increase the number of well-resolved peptides. Modify the chromatographic gradient and time to improve separation and resolution of pepsin fragment peptides.
2. Add reducing agents such as tris(2-carboxyethyl)phosphine (TCEP) or dithiothreitol (DTT) in quench solutions for better proteolytic cleavage of proteins that have disulphide bonds.
3. Incubate quenched samples with denaturants such as urea/guanidium-HCl (which helps to unfold the protein for optimal proteolytic cleavage) to improve primary sequence coverage.
4. Improve data resolution by optimizing the protocol to generate multiple overlapping and nested peptides.
   NOTE: Estimated time required for a single LC/MS experiment is 20 min and is dependent on the LC gradient time. Four deuterium labelling time points and an undeuterated sample experiment are together estimated to take 3 - 4 h per individual experimental replicate, per ligand, or fragment-bound or ligand-free condition. LC/MS data collection time for three individual replicates for each fragment or ligand binding condition is expected to be 9 - 12 h.

## 5. Deuterium Exchange Reaction of High-Affinity Ligand-Protein Interaction to Identify Peptide-Reporters

1. Prepare deuterium exchange reactions of ligand-free Hsp90 by addition of 1 µL of 100 µM Hsp90 protein solution (step 1.1) + 2 µL DMSO-blank + 27 µL of Hsp90 $D_2O$ buffer (step 1.2) resulting in a final labelling $D_2O$ concentration of 90% and Hsp90 concentration of 3.3 µM.
2. Prepare similar deuterium exchange reactions of high-affinity inhibitor-bound Hsp90 protein by adding 1 µL of Hsp90 protein solution (step 1.1) + 2 µL high-affinity inhibitor solution (radicicol and 17-AAG from step 1.4.1) + 27 µL of Hsp90 $D_2O$ buffer (step 1.2) resulting in a final labelling $D_2O$ concentration of 90% and Hsp90 concentration of 3.3 µM.
3. Perform deuterium exchange reactions by incubating deuterium exchange reactions (steps 5.1 and 5.2) for specific deuterium labelling time-points (0.5 min, 1 min, 2 min, 5 min and 10 min).
4. Include additional deuterium exchange time-points such as 100 min and 24 h, if needed. Include millisecond deuterium exchange reactions with a stopped-flow instrument, if required.
   NOTE: A deuterium exchange reaction for Hsp90 was carried out for the following deuterium labelling times: t= 0.5, 1, 2, 5, and 10 min. Although, this time series represents a shorter labeling time series for deuterium exchange, this was the optimal labeling-time-window where the largest changes were observed.
5. Add the prepared Hsp90 quench solution (step 1.5) to quench the deuterium exchange reaction by reducing the pH to 2.5. Inject quenched samples to liquid chromatography coupled to a mass spectrometer (LC/MS) setup (step 3.2).
6. Analyze the peptides in the peptide-list (step 3.7) and determine deuterium uptake values for each peptide in all the experimental conditions: ligand-free Hsp90 (step 5.1) and high-affinity inhibitor-bound Hsp90 (step 5.2). Calculate deuterium uptake values for each peptide at each of the deuterium labelling time-points (step 5.3).
7. Compare deuterium uptake values for peptides and calculate differences in deuterium uptake for each peptide, between ligand-free Hsp90 and high-affinity-bound Hsp90.
8. Filter peptides that show significant differences in deuterium uptake above the significance threshold of 0.5 Da.
9. Identify Hsp90 residues involved in ligand binding by analyzing ligand-bound structures of Hsp90 from PDB.
   1. Determine residues within 4 Å distance from the ligand using a structure visualization tool such as PyMOL and classify them as orthosteric residues. Load the protein-ligand complex structure in PyMOL using the PDB identifier 4EGK for the Hsp90-Radicicol structure. Click and select the ligand radicicol (RDC) in the sequence and use the action menu to modify the selection to include residues within 4 Å distance. Classify these amino-acids as orthosteric residues.
   2. Additionally, include residues that have been annotated as binding sites for the ligand (in either PDB or literature)[22].
   3. Determine the list of peptides in Hsp90 that show significant differences (>0.5 Da) in deuterium uptake between the ligand-free and ligand-bound states.
10. Classify peptides that show significant differences from step 5.9 and span one or more orthosteric residues as orthosteric reporter-peptides.
11. Classify peptides that show significant differences from step 5.9 but do not include any orthosteric residues as allosteric reporter-peptides.
    NOTE: Changes at these peptides represent long-range allosteric changes in response to ligand binding at orthosteric sites.

## 6. Deuterium Exchange Reactions of Fragment-Protein Interactions to Determine Orthosteric and Allosteric Effects due to Fragment-Binding to Hsp90

1. Prepare deuterium exchange reactions of fragment-bound Hsp90 by addition of 1 µL of 100 µM Hsp90 protein solution (step 1.1) + 2 µL of fragment solutions in DMSO (Fragment 1 and 2 from step 1.4.2) + 27 µL of Hsp90 $D_2O$ buffer (step 1.2) resulting in a final labelling $D_2O$ concentration of 90% and Hsp90 concentration of 3.3 µM and fragment concentration of 20 mM.
2. Select a small-set of suitable deuterium labelling time-points (30 s and 5 min) which show the highest changes in high-affinity-ligand-protein interactions.
3. Preferably include shorter deuterium labelling time-points (30 s), since differences in deuterium uptake upon fragment-binding are readily apparent at these short deuterium labelling time-points due to the weak binding affinities of fragment compounds.
4. Perform deuterium exchange reactions for fragment-Hsp90 interactions by incubating the deuterium exchange reactions (step 6.1) for the specific time points (30 s and 5 min), followed by addition of Hsp90 quench solution to reduce the pH to 2.5.
5. Determine deuterium uptake values (similar to step 5.7) for orthosteric and allosteric reporter-peptides identified in steps 5.10.3 and 5.11.
6. Analyze fragment-protein interaction data at these reporter-peptides to qualitatively determine the orthosteric and allosteric effects of fragment-binding based on the number of peptides or regions that show changes upon each fragment binding.
7. Quantitate these changes by measuring the differences in deuterium uptake at each of these reporter-peptides. The differences indicate the amount of protection at these reporter-peptides due to fragment-binding and indirectly report the strength of the interaction[10].
8. Identify reporter-peptides that show significant differences in deuterium uptake above the significance threshold of 0.5 Da (similar to 5.10). Determine the number of orthosteric and allosteric peptides that show significant differences upon fragment-binding for each fragment (Fragment 1 and 2, similar to 5.11 and 5.12).

## 7. Additional Interpretation

1. Analyze the deuterium uptake kinetics over time to predict the relative $k_{off}$ rates for ligands (or fragments) with similar dissociation constants ($K_D$). Measure decreases in observed deuterium uptake differences (ligand-bound protein versus ligand-free protein) with increases in deuterium labelling time.
2. Compare dissociation rates ($k_{off}$) of ligands and rank them based on faster observed decreases in deuterium uptake differences with increases in deuterium labelling times at orthosteric reporter-peptides.
3. Identify ligands with faster dissociation rates by comparing those that show earlier decreases in deuterium uptake differences with increases in deuterium labelling time at orthosteric reporter-peptides.

NOTE: Estimated time for data analysis can be from 2 - 10 days and is dependent on the number of fragments or ligands analyzed.

## Representative Results

In order to identify the reporter peptides that represent changes in Hsp90 upon ligand binding, changes in deuterium uptake were quantified for Hsp90 in the presence and absence of the high affinity ligands. Differences in deuterium uptake were determined at pepsin-proteolyzed peptides between the high-affinity-ligand bound-Hsp90 and ligand-free-Hsp90 and reporter peptides that showed significant differences in deuterium uptake (>= 0.5 Da) were identified. The error in a single deuterium exchange experiment has been shown to be 0.17 Da[40]. This is a composite of variability in pH, temperature, samples, and instrumentation. The maximum standard error in a subtractive analysis is twice that - 0.34 Da. Hence, a threshold of 0.5 Da was set for any difference to be considered significant. Among all the reporter peptides that showed ligand-specific changes, orthosteric reporter peptides were determined using crystallographic structural information. Peptides that span residue(s) within a 4 Å H-bonding distance, or annotated to be part of the binding pocket by PDB, are considered as orthosteric reporter peptides and monitor changes at the binding site. For Hsp90, multiple residues were annotated in PDB to make contacts with the ligand in the orthosteric binding pocket. Peptides spanning residues L48, N51, D54, A55, and K58 were classified as orthosteric peptides in region O1 since these residues were shown to be involved in direct binding to the ligand. Similarly, orthosteric regions O2 spanned residues D93, I96, M98, D102, N106, L107 and K112, region O3 with residues G135, V136, G137 and F138 and region O4 with residues T184 and V186 that are known to make orthosteric contacts with the ligand. Peptides spanning these residues were classified as orthosteric reporters (**Figure 1**). Peptides that showed significant differences, but are not part of the orthosteric regions, are considered allosteric reporter peptides and monitor changes at the allosteric site. For instance, peptide spanning residues 62-76 showed differences in deuterium uptake between the ligand-bound and ligand-free Hsp90 although the residues involved do not have orthosteric binding contacts with the ligand, hence the changes observed in this peptide locus were classified as representing allosteric changes that are distal to the binding site. High-affinity ligands are used to identify these orthosteric and allosteric reporter peptides (**Figure 1**). A protein-wide difference plot is used to determine the entire set of reporter peptides (orthosteric and allosteric) across Hsp90. These clearly show four distinct orthosteric and allosteric regions represented by multiple reporter peptides (**Figure 2**). Mapping these regions on the structure of Hsp90 show that the orthosteric regions (colored blue) surround the ligand-binding pocket, while allosteric regions are distal to the binding site (**Figure 2**). A few orthosteric reporter peptides are sensitive enough to capture differences between the binding kinetics of the two high-affinity ligands (Orthosteric reporter peptide I, **Figure 1**).

Kinetics of deuterium exchange indicate that the early time points of exchange show the highest magnitude differences in deuterium exchange and these differentially drop with increasing deuteration times, dependent on the ligand dissociation rates ($k_{off}$) (**Figure 2**). Hsp90-Fragment interactions showed the largest differences at labelling time-points up to 10 min, specifically at 30 s and 5 min. Some peptide reporters showed decreased differences at time-points after 10 min due to fast $k_{off}$ rates of fragments. HDXMS data (**Figure 2**) showed that the faster decreases in difference in deuterium uptake for 17-AAG (bottom-panel, **Figure 2**) compared to radicicol (top-panel), over increased deuterium labelling time, suggesting that 17-AAG dissociates faster than radicicol despite their similar dissociation constants ($K_D$). A higher magnitude of difference in deuterium exchange observed in radicicol-Hsp90 complex compared to 17-AAG-Hsp90 complex also suggests the radicicol makes additional or stronger contacts at the orthosteric binding site (Orthosteric region O2, **Figure 2**, data from[22]).

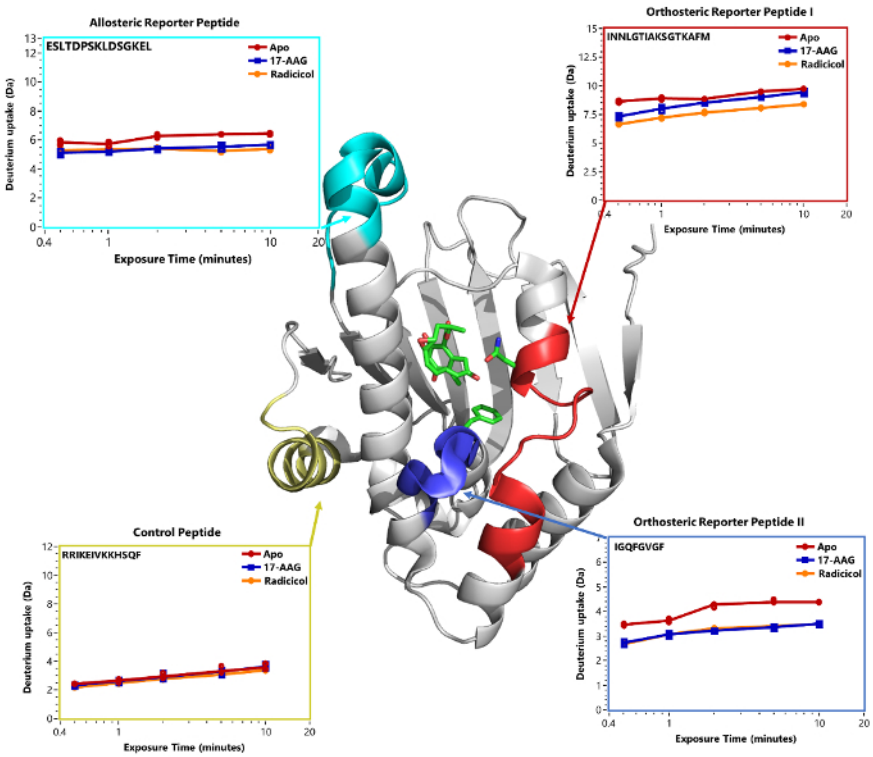


**Figure 1: Identification of reporter peptides for monitoring orthosteric binding and allosteric effects.** Comparison of deuterium uptake values between the ligand-bound-Hsp90 and apo-Hsp90 shows changes at distinct regions in the protein. Representative pepsin-proteolyzed peptides and their differences in deuterium uptake are shown from four different regions of Hsp90 upon binding two high affinity ligands (Radicicol and 17-AAG). Orthosteric reporter peptides contain residues (side chains represented as sticks) in the binding sites that make orthosteric contacts (Orthosteric reporter peptide I and II). These orthosteric peptides show differences in deuterium uptake upon ligand binding. Comparing these orthosteric peptides, peptide I (boxed red and colored red on the structure of Hsp90) is able to differentiate between the two ligands, while changes in peptide II (boxed in blue and colored blue on the structure of Hsp90) are similar for both the ligands in the deuterium labelling time-points observed. A representative allosteric reporter peptide (boxed in cyan and colored cyan on the structure of Hsp90) shows changes in deuterium uptake upon ligand binding and does not contain any residue which makes orthosteric contacts with the ligand and is distal to the binding site. These changes in this allosteric reporter peptide are allosteric changes due to ligand binding. A control peptide (boxed in yellow and colored yellow on the structure of Hsp90) is shown, which neither involved in orthosteric binding nor shows any distal allosteric changes. Deuterium uptake plots for the highlighted reporter peptides are represented in boxes. The deuterium uptake values (Y-axis in Daltons) are plotted against their deuterium labelling times (logarithmic X-axis) for at least three independent HDXMS experiments in each set of conditions and colored according to key. The reporter peptides residues are mapped on to the structure of Hsp90 (grey). Radicicol bound at the ligand binding pocket is shown as green sticks (PDB ID: 4EGK). (Figure adapted from[22]) Please click here to view a larger version of this figure.

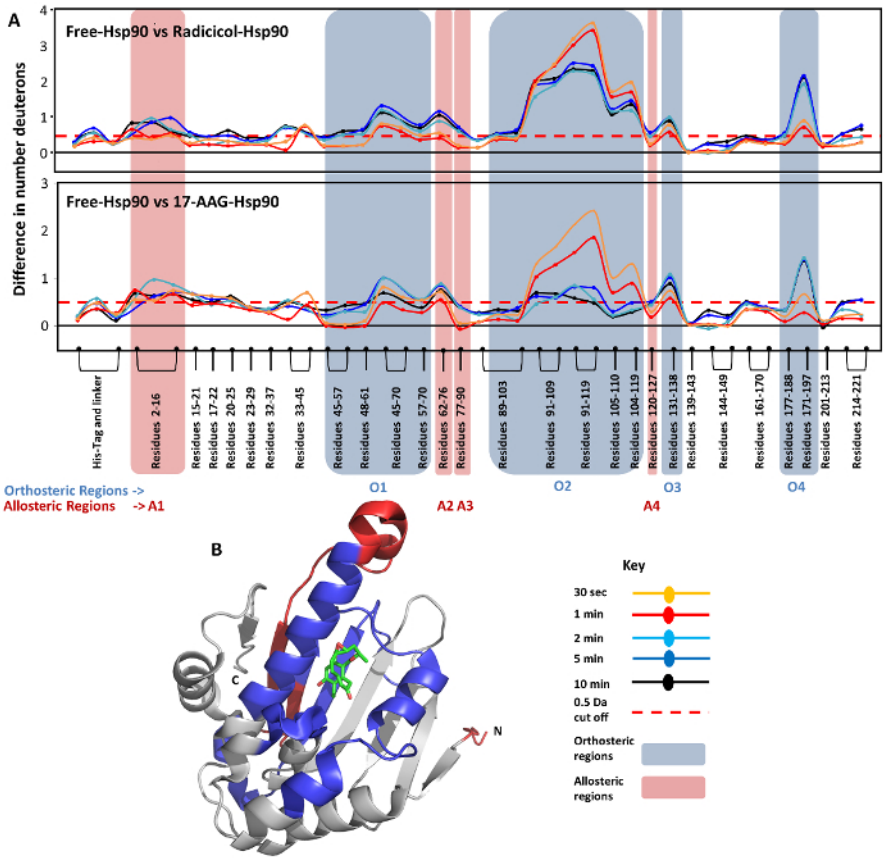


**Figure 2: Dissecting orthosteric and allosteric changes in Hsp90.** A plot of differences in deuterium exchange at reporter peptides upon ligand binding across Hsp90 shows orthosteric regions that show changes and distal sites that show allosteric effects. **(A)** The absolute difference in numbers of deuterons (Y-axis) between the free and ligand bound-Hsp90 is plotted for each pepsin digest fragment listed from the N to the C terminus (x-axis) for each deuterium exchange time point (t = 0.5, 2, 5, 10 min) in a 'difference plot'. Shifts in the positive scale represent decreases in deuterium exchange and shifts in the negative scale represent increases in deuterium exchange when compared to apo-Hsp90. Regions showing significant differences above a threshold of 0.5 Da (red dashed line) are compared with orthosteric sites (blue boxes) to predict allosteric regions. Peptides (highlighted in red) show regions with differences in distal allosteric regions, which are not involved in orthosteric binding. Peptides spanning these regions (marked in red boxes) are divided into four allosteric regions A1 to A4. Radicicol and 17-AAG showed differences in A1 and A2, while only radicicol showed changes in A3 and A4. Time points are colored according to key. **(B)** Predicted allosteric regions are mapped on to the structure of Hsp90 (red), together with the orthosteric regions, in blue. Radicicol bound at the ligand binding pocket is shown as sticks (PDB ID: 4EGK). (Figure adapted from[22]) Please click here to view a larger version of this figure.

Reporter peptides identified from high-affinity-ligand analysis (in both orthosteric and allosteric regions) are used to monitor changes across Hsp90 in response to fragment binding. Fragments mediate contacts across all the orthosteric contacts observed with high affinity ligands, but the magnitude of difference and time-dependent differences are considerably lower (**Figure 3**, data from [22]). Fragments can be compared and ranked in terms of their magnitude of differences, the number of orthosteric regions where changes are observed, and the time-dependent increases or decreases in deuterium uptake. Each of these can be represented as below: Both fragments 1 and 2 show significant changes in all four orthosteric sites and the four allosteric sites observed in high affinity ligands. However, fragment 1 shows changes at an additional allosteric peptide at region A5 (colored orange in **Figure 3**). Furthermore, fragment 1 shows higher magnitude changes in regions O1, O4, A1, A3 and A4, compared to fragment 2. Kinetics of deuterium uptake also show that changes due to fragment 1 at orthosteric site O2 are observable until the 10 min deuterium labelling time-point, compared to fragment 2, where there are no significant changes observable after 30 s of deuterium exchange. These results suggest that this method of monitoring low-affinity fragments and the changes (orthosteric and allosteric) using HDXMS allows the comparison and ranking of ligands and fragments based on their binding and allosteric effects in solution.

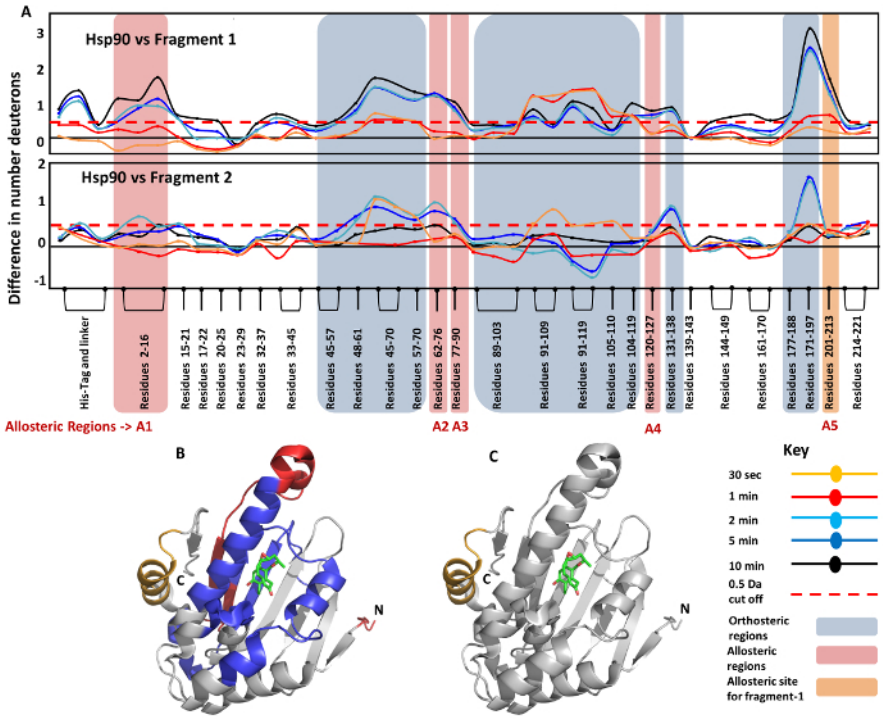


**Figure 3: Fragments 1 and 2 differ in the nature of their allosteric effects on Hsp90. (A)** The absolute difference in numbers of deuterons (inferred from the difference in mass in Daltons (Da)) (Y-axis) between the free and ligand bound state is plotted for each pepsin digest fragment, listed from the N to the C terminus (X-axis) of Hsp90 for each deuterium exchange time point (t = 0.5, 2, 5, 10 min) in a 'difference plot'. Shifts in the positive scale represent decreases in deuterium exchange and shifts in the negative scale represent increases in deuterium exchange when compared to the apo-Hsp90. Regions showing significant differences above a threshold of 0.5 Da (red dashed line) are compared with orthosteric sites (blue boxes) to establish allosteric regions (red boxed). Fragment 2 does not show any changes in region A4, similar to 17-AAG, while fragment 1 shows differences, similar to Radicicol. In addition, fragment 1 shows an allosteric response at region A5 (residues 201-213 shown in orange box), which is not observed in the other three ligands. Time points are colored according to the key. **(B, C)** The identified orthosteric (blue) and allosteric regions (red) for fragments are mapped on to the structure of Hsp90 in blue. **(C)** The changes in allosteric site A5 in Hsp90 are observed only for fragment 2 (highlighted in orange). Radicicol bound at the ligand binding pocket is shown as sticks (PDB ID: 4EGK). (Figure adapted from[22]) Please click here to view a larger version of this figure.

## Discussion

**Critical steps in the protocol:** It is essential that the pH of solutions, including protein buffers and LC-solutions, are all maintained at a pH of 2.5 to minimize loss of deuterium labelling. It is also critical that deuterium exchange experiments be carried out at saturating concentrations of ligands to maintain a homogenous population of ligand-bound protein. This can be estimated from the ligands' or fragments' dissociation constants and need to be consistent among all fragment-protein deuterium exchange experiments. Identification of reporter peptides should involve differences in deuterium uptake, together with a detailed structural characterization of residue-wise bonding contacts at the ligand-protein interface to identify peptides that contained at least one non-hydrogen atom proximal to the ligand and are thus involved in ligand binding. Spatially distal peptides showing changes in deuterium uptake need to be carefully examined to exclude regions with orthosteric ligand contacts.

**Modifications and troubleshooting:** The observed differences at reporter peptides represent composite changes due to ligand binding and include both orthosteric changes at the binding site and allosteric changes at the ligand-binding site. Any known structural information on additional co-factors and partner binding sites can be defined as allosteric regions which have been reported earlier to respond to ligand binding. Finding the optimal deuterium exchange and ligand concentrations can be a challenge. It is advisable to utilize deuterium uptake profiles of ligand-free-protein to optimize the deuterium labelling times and to preferentially pick the shortest labelling times, in case there is a lack of differences between them. In case of availability of structural information in homologous proteins or other ligands, these are also likely to provide important clues in terms of dissociation constants, multiple binding sites, and any observable conformational changes.

**Limitations of the method:** HDXMS is extremely sensitive to changes in protein conformation and offers a perturbation map for fragment and ligand binding to the target proteins. One limitation is that it provides this map at a peptide resolution. The authors wish to emphasize that HDXMS when combined with X-ray crystallography can provide important complementary insights into dynamics of protein-ligand interaction. Hence, this method is also most suited to study protein-ligand systems where structural information about orthosteric contacts is available. The availability of high-resolution structural information eases prediction and separation of allosteric effects from orthosteric contact points. Additionally, the resolution of this approach depends on the ability to obtain pepsin-proteolyzed reporter peptides that span the orthosteric and allosteric sites to monitor conformational changes. Changes observed in longer peptides (>15 residues in length) lack the resolution to accurately localize changes. However, shorter, overlapping and nested peptides (<10 residues in length) from commercially available high-pressure pepsin proteolysis can overcome these limitations.

**Significance of the method with respect to existing alternative methods:** Dynamics is a major consideration of allosteric processes in proteins and represents a challenge for biophysical and structural characterization of conformational changes. Additionally, fragments with weak dissociation constants mediate transient interactions and are difficult to capture due to their high $k_{off}$ rates. Since deuterium exchange reactions are initiated by mixing a ligand and its target protein with deuterated buffer, it is possible to capture steady-state and equilibrium kinetics from a range of deuterium labelling times. The ability to distinguish between similar high-affinity ligands and fragments based on the magnitude and kinetics of deuterium exchange differences has been demonstrated in the results section. In addition, HDXMS has especially important implications in drug and fragment screening in proteins that are challenging to crystallize due to factors such as aggregation. This method is uniquely poised to provide a comprehensive description of protein-ligand complexes: structural localization of binding, allostery, and kinetic information on the relative $k_{on}$ and $k_{off}$ rates. These applications have enabled HDXMS to become an emerging tool in small-molecule and biopharmaceutical discovery[15-17].

**Future applications or directions of the method:** An extension of monitoring changes in protein-fragment interactions is the ability for this approach to be utilized as an efficient fragment screening method. The magnitude of deuterium exchange difference and kinetics of difference observed directly reports on fragment efficacy. It is hence possible to rank-order fragments based on: 1) Number of loci or peptides showing differences in deuterium exchange. 2) Magnitude of difference at each of these loci. 3) Reduction in differences over deuterium labelling time. These offer a HDXMS framework for iterative fragment screening and optimization in the FBLD pipeline. Optimization of lead-compound by monitoring differences due to modification of multiple single moieties can be used to preferentially optimize some components of the lead-compound vs the others. Overall, the method demonstrated here is expected to accelerate fragment-based drug discovery.

## Disclosures

The authors declare that they have no competing or financial interests.

## Acknowledgements

This work was supported by a grant from Singapore Ministry of Education Academic research fund-Tier 3 (MOE2012-T3-1-008) and Tier1.

## References

1. Renaud, J.P. *et al.* Biophysics in drug discovery: impact, challenges and opportunities. *Nat Rev Drug Discov.* **15** (10), 679-698 (2016).
2. Hajduk, P.J., & Greer, J. A decade of fragment-based drug design: strategic advances and lessons learned. *Nat Rev Drug Discov.* **6** (3), 211-219 (2007).
3. Congreve, M., Carr, R., Murray, C., & Jhoti, H. A 'rule of three' for fragment-based lead discovery? *Drug Discov Today.* **8** (19), 876-877 (2003).
4. Motlagh, H.N., Wrabl, J.O., Li, J., & Hilser, V.J. The ensemble nature of allostery. *Nature.* **508** (7496), 331-339 (2014).
5. Boehr, D.D., Nussinov, R., & Wright, P.E. The role of dynamic conformational ensembles in biomolecular recognition. *Nat Chem Biol.* **5** (11), 789-796 (2009).
6. Patching, S.G. Surface plasmon resonance spectroscopy for characterisation of membrane protein-ligand interactions and its potential for drug discovery. *Biochim Biophys Acta.* **1838** (1 Pt A), 43-55 (2014).
7. Shah, N.B., & Duncan, T.M. Bio-layer interferometry for measuring kinetics of protein-protein interactions and allosteric ligand effects. *J Vis Exp.* (84), e51383 (2014).
8. Nussinov, R., & Tsai, C.J. Unraveling structural mechanisms of allosteric drug action. *Trends Pharmacol Sci.* **35** (5), 256-264 (2014).
9. Cui, Q., & Karplus, M. Allostery and cooperativity revisited. *Protein Sci.* **17** (8), 1295-1307 (2008).
10. Chandramohan, A., Tulsian, N.K., & Anand, G.S. Dissecting Orthosteric Contacts for a Reverse-Fragment-Based Ligand Design. *Anal Chem.* (2017).
11. Miyashita, O., Onuchic, J.N., & Wolynes, P.G. Nonlinear elasticity, proteinquakes, and the energy landscapes of functional transitions in proteins. *Proc Natl Acad Sci U S A.* **100** (22), 12570-12575 (2003).
12. Okazaki, K., & Takada, S. Dynamic energy landscape view of coupled binding and protein conformational change: induced-fit versus population-shift mechanisms. *Proc Natl Acad Sci U S A.* **105** (32), 11182-11187 (2008).
13. Englander, S.W., & Kallenbach, N.R. Hydrogen exchange and structural dynamics of proteins and nucleic acids. *Q Rev Biophys.* **16** (4), 521-655 (1983).
14. Pacholarz, K.J., Garlish, R.A., Taylor, R.J., & Barran, P.E. Mass spectrometry based tools to investigate protein-ligand interactions for drug discovery. *Chem Soc Rev.* **41** (11), 4335-4355 (2012).
15. Deng, B., Lento, C., & Wilson, D.J. Hydrogen deuterium exchange mass spectrometry in biopharmaceutical discovery and development - A review. *Anal Chim Acta.* **940**, 8-20 (2016).
16. Lee, J.J., Park, Y.S., & Lee, K.J. Hydrogen-deuterium exchange mass spectrometry for determining protein structural changes in drug discovery. *Arch Pharm Res.* **38** (10), 1737-1745 (2015).
17. Marciano, D.P., Dharmarajan, V., & Griffin, P.R. HDX-MS guided drug discovery: small molecules and biopharmaceuticals. *Curr Opin Struct Biol.* **28**, 105-111 (2014).
18. Schmidt, C., & Robinson, C.V. Dynamic protein ligand interactions--insights from MS. *FEBS J.* **281** (8), 1950-1964 (2014).
19. Edink, E. *et al.* Fragment growing induces conformational changes in acetylcholine-binding protein: a structural and thermodynamic analysis. *J Am Chem Soc.* **133** (14), 5363-5371 (2011).
20. Henzler-Wildman, K.A. *et al.* A hierarchy of timescales in protein dynamics is linked to enzyme catalysis. *Nature.* **450** (7171), 913-916 (2007).
21. Hoofnagle, A.N., Resing, K.A., & Ahn, N.G. Protein analysis by hydrogen exchange mass spectrometry. *Annu Rev Biophys Biomol Struct.* **32**, 1-25 (2003).
22. Chandramohan, A. *et al.* Predicting Allosteric Effects from Orthosteric Binding in Hsp90-Ligand Interactions: Implications for Fragment-Based Drug Design. *PLoS Comput Biol.* **12** (6), e1004840 (2016).

 

23. Krishnamurthy, S. *et al.* Distinguishing direct binding interactions from allosteric effects in the protease-HK97 prohead I delta domain complex by amide H/D exchange mass spectrometry. *Bacteriophage.* **4** (4), e959816 (2014).
24. Murray, C.W. *et al.* Fragment-based drug discovery applied to Hsp90. Discovery of two lead series with high ligand efficiency. *J Med Chem.* **53** (16), 5942-5955 (2010).
25. Solit, D.B., & Rosen, N. Hsp90: a novel target for cancer therapy. *Curr Top Med Chem.* **6** (11), 1205-1214 (2006).
26. Brough, P.A. *et al.* Combining hit identification strategies: fragment-based and in silico approaches to orally active 2-aminothieno[2,3-d]pyrimidine inhibitors of the Hsp90 molecular chaperone. *J Med Chem.* **52** (15), 4794-4809 (2009).
27. Huth, J.R. *et al.* Discovery and design of novel HSP90 inhibitors using multiple fragment-based design strategies. *Chem Biol Drug Des.* **70** (1), 1-12 (2007).
28. Prodromou, C. *et al.* Identification and structural characterization of the ATP/ADP-binding site in the Hsp90 molecular chaperone. *Cell.* **90** (1), 65-75 (1997).
29. Austin, C. *et al.* Fragment screening using capillary electrophoresis (CEfrag) for hit identification of heat shock protein 90 ATPase inhibitors. *J Biomol Screen.* **17** (7), 868-876 (2012).
30. Stebbins, C.E. *et al.* Crystal structure of an Hsp90-geldanamycin complex: targeting of a protein chaperone by an antitumor agent. *Cell.* **89** (2), 239-250 (1997).
31. Roughley, S.D., & Hubbard, R.E. How well can fragments explore accessed chemical space? A case study from heat shock protein 90. *J Med Chem.* **54** (12), 3989-4005 (2011).
32. Hentze, N., & Mayer, M.P. Analyzing protein dynamics using hydrogen exchange mass spectrometry. *J Vis Exp.* (81) (2013).
33. Wang, L.C., Krishnamurthy, S., & Anand, G.S. In: *Hydrogen Exchange Mass Spectrometry of Proteins.* John Wiley & Sons, Ltd, 19-35 (2016).
34. Badireddy, S. *et al.* Cyclic AMP analog blocks kinase activation by stabilizing inactive conformation: conformational selection highlights a new concept in allosteric inhibitor design. *Mol Cell Proteomics.* **10** (3), M110 004390 (2011).
35. Li, G.Z. *et al.* Database searching and accounting of multiplexed precursor and product ion spectra from the data independent analysis of simple and complex peptide mixtures. *Proteomics.* **9** (6), 1696-1719 (2009).
36. Geromanos, S.J. *et al.* The detection, correlation, and comparison of peptide precursor and product ions from data independent LC-MS with data dependant LC-MS/MS. *Proteomics.* **9** (6), 1683-1695 (2009).
37. Pascal, B.D. *et al.* HDX workbench: software for the analysis of H/D exchange MS data. *J Am Soc Mass Spectrom.* **23** (9), 1512-1521 (2012).
38. Rey, M. *et al.* Mass spec studio for integrative structural biology. *Structure.* **22** (10), 1538-1548 (2014).
39. Pascal, B.D. *et al.* The Deuterator: software for the determination of backbone amide deuterium levels from H/D exchange MS data. *BMC Bioinformatics.* **8**, 156 (2007).
40. Houde, D., Berkowitz, S.A., & Engen, J.R. The utility of hydrogen/deuterium exchange mass spectrometry in biopharmaceutical comparability studies. *J Pharm Sci.* **100** (6), 2071-2086 (2011).


 